Electron-hole droplet transport up to near-sonic velocity in Si

M. A. Tamor and J. P. Wolfe
Physics Department and Materials Research Laboratory, University of Illinois at Urbana-Champaign, Urbana, Illinois 61801
(Received 21 June 1982; revised manuscript received 18 August 1982)

In the past, several interesting effects have been observed in conducting systems where the carrier drift velocity is made to exceed the sound velocity. Nonlinear momentum damping and phonon amplification have been demonstrated in several materials (CdS,Ge, PbTe). However, high drift velocities with a high density of carriers produce immense current densities, which cause very rapid carrier and sample heating. This heating limits such transport studies to very short current pulses. In contrast, a dense, high-mobility system of photoexcited carriers in ultrapure Si allows more complete study of the near-sonic transport regime. The electron-hole liquid which condenses at low temperatures is a highly degenerate conductor. The liquid takes the form of electron-hole droplets (EHD's) of micrometer size and fixed density. The total amount of conducting volume is thus controlled by excitation level. The low carrier density (relative to a metal) and small volume of the liquid, together with the high droplet mobility, tremendously reduce the rate of sample heating by carrier-phonon scattering, compared to a normal metal. In our experiments, with $T \lesssim 2.1$ K, the electrically neutral EHD's are accelerated by a strain-induced gradient in the semiconductor energy gap $E_g(x)$. The energy shift of the recombination luminescence peak gives the motive force per pair, $F_\sigma = -dE_g/dx$. In this paper we report basic measurements of the EHD mobility in Si. The measured drift velocity v_d is found to be proportional to F_σ as long as v_d is much less than the sound velocity S. We further find that the momentum damping rate, $\tau^{-1} = F_\sigma/mv_d$, increases as S is approached. For $v_d < 0.9S$ the observed damping is consistent with a theory describing the absorption and re-emission of thermal phonons (D'yakanov and Subashiev, 1978). At low velocity the observed droplet mobility exhibits the rapid T dependence predicted by the Bloch conductivity theory for a degenerate Fermi liquid. The data show a saturation in v_d at $0.9S$ that indicates a sharp increase in damping. The thermal-phonon scattering theory does not predict such a velocity limit. However, a "sound barrier," due to the Cherenkov-type emission of phonons when $v_d \geq S$, has been predicted. We propose that the observed velocity saturation is due to this effect.

I. INTRODUCTION

The electrical conductivity of metals is generally dominated at room temperature by collisions of carriers with lattice phonons and, at low temperatures ($T \lesssim 20$ K), by collisions with impurity atoms and crystal defects.[1] Modern materials fabrication techniques provide crystals of such perfection and purity that the carrier-phonon interaction is still dominant at temperatures as low as 1 K.[2] Many interesting conductivity effects are expected when a highly degenerate Fermi system is accelerated to the phonon velocity. The conductivity may drop drastically, and the system of carriers may be driven out of thermal equilibrium to a temperature higher,[3] or more interestingly, lower than that of the lattice.[4] Furthermore, net acoustic gain has been observed for phonons traveling parallel to the direction of drift, presenting the possibility of producing a phonon maser.[5,6]

There is a major obstacle in the path of producing a near-sonic drift velocity: The current densities produced are generally so large that the conducting material rapidly heats up, making continuous measurements impossible. The classical conductivity relations state the conductivity $\sigma = ne\mu$ in terms of the mean carrier mobility $\mu \equiv v_d/E = e\tau/m$, where v_d is the drift velocity, E the electric field, n the carrier density, τ the carrier momentum damping time, and m the effective carrier mass. The current density is given by $J = \sigma E = nev_d$. In ordinary metal a drift velocity near the sound velocity will produce a current density $J_s = neS \approx 10^9$ A/cm^2, where S is the sound

velocity. These very large currents can be attained only for very short times (~ 1 nsec) in very thin samples (2 μm diameter whiskers).[7]

To take another approach, a semiconductor may be doped to such an extent that it becomes a metallic conductor ($n \gtrsim 10^{17}$ cm^{-3}). High-velocity transport in such Si and Ge has been extensively studied.[8] Electron drift velocities up to 10^7 cm/sec have been observed. However, it was clear that the carriers in those systems are heated far above the ambient lattice temperature. For this relatively low density ($\sim 10^{17}$ cm^{-3} compared with 10^{23} cm^{-3} for a metal) and elevated temperature, these carriers are essentially a nondegenerate gas (with $kT \gg E_f$, the Fermi energy), termed the "hot-electron" system. Electrons injected by a pulsed electron beam into purer material also exhibit hot-carrier effects.

Current saturation in the piezoelectric semiconductors CdS and PbTe has been observed, again in a pulsed mode.[5,9] The limiting velocity was near that of sound. In CdS and Ge acoustic gain for phonons transmitted along the current flow was observed.[6,10] However, the prolongation of the current pulse resulted in damage to the sample.

It is apparent from the above experiments that a highly degenerate conducting system with very small thermal dissipation to the crystal lattice may allow observation of several unusual effects in electronic transport. The droplets of electron-hole liquid (EHL) produced by photoexcitation of very pure silicon at low temperature satisfy these criteria.

The general properties of EHL are described at length in Ref. 11. The electron-hole liquid is a condensed phase of electron-hole pairs in a semiconductor. The carriers form two interpenetrating Fermi fluids—electrons and holes. The liquid is electrically neutral. In very pure Si the EHL can be produced at temperatures below a critical temperature $T_c \approx 27$ K and has an electron-hole pair density $n_0 \simeq 3 \times 10^{18}$ cm^3.[12] The liquid appears in the form of tiny electron-hole droplets (EHD) with radii less than 1 μm and a recombination lifetime of 140 nsec. The carriers inside the drop form the conducting system of interest.

Because the EHD is an intrinsic state of the pure semiconductor, the purest material may be used, minimizing carrier-impurity interactions. Above the threshold of droplet production, the photoexcitation level determines the number of droplets produced (i.e., the total volume of liquid) and does not affect the electron-hole-pair density within the drops. Thus a variable total volume may be produced as desired. Even at the highest excitation levels, the filling factor (volume fraction actually occupied by EHD) does not exceed 1%.[13] At sonic velocities the equivalent current density (actually carrier flux, as the drops are neutral) is then given by $0.01neS = 10^3$ A/cm^2. Thus sonic drift of EHD corresponds to a millionfold current reduction from ordinary metal, and a hundredfold reduction from the doped semiconductor.

The energy per unit volume dissipated to the lattice by each of the three conducting systems may also be estimated

$$P = nFv_d = nmv_d^2/\tau \tag{1}$$

where $F = mv_d/\tau$ is the force per particle required to drive the carriers at a drift velocity v_d. For an ordinary metal $\tau \approx 10^{-11}$ sec and $P \sim 10^{18}$ erg/cm^3 sec at 2 K. For EHD in Si at 2.0 K we estimate $P \sim 10^{10}$ erg/cm^3 sec. The energy dissipations, currents, and drift forces for the conducting systems mentioned above are compared in Table I. The estimates for EHD assume that $\tau \sim 10^{-9}$ sec, which is the measured scattering time for free excitons (FE) in Si.[14] In short, the EHD in Si is a degenerate Fermi system for which the continuous transport of carriers at sonic velocity is possible without the heating constraints found in metals and doped semiconductors.

On the other hand, it is not possible to examine the transport of EHD with the techniques used in ordinary conductivity studies. The EHD carries no net charge, and so is not accelerated in an electric

TABLE I. Comparison of carrier drift properties of three conducting systems: metal, doped semiconductor, and electron-hole droplets in silicon. The system parameters are carrier density n_0, sound velocity S, and carrier scattering time τ. Using these values we compute the motive force F_S required for a sonic drift velocity, and the corresponding current density J_S and power dissipation P_S.

	Cu (2 K)	Si (77 K)[a]	EHD (2 K)
n_0 (cm^{-3})	10^{23}	10^{17}	0.01×10^{18} [b]
S (cm/sec)	2×10^5	5×10^5	5×10^5
τ (sec)	10^{-11}	10^{-11}	10^{-9}
F_S (eV/cm)	10^2	10^2	10^0
J_S (A/cm^2)	10^9	10^5	10^3
P_S (erg/cm^3 sec)	10^{18}	10^{12}	10^{10}

[a]Carriers contributed by doping freeze out at temperatures below 77 K. Also, impurity scattering with dopant-atoms-limits mobility at lower temperatures.
[b]1% filling factor (see text and Ref. 13).

field. This handicap is overcome by applying a nonuniform crystal stress to generate a gradient in semiconductor band gap. This strain-gradient method was used in Refs. 14 and 15 and will be further explained below. Using the drift relation ($F=mv_d/\tau$) and $\tau\approx10^{-9}$ sec, we have estimated the force required to achieve near-sonic EHD transport in Table I. With $m=0.5\times10^{-27}$ g, $v_d=5\times10^5$ cm/sec, and $\tau\simeq1$ nsec, we have $F=3\times10^{-13}$ dyne/*e-h* pair, which is equivalent to an electric field F/e of only 0.2 V/cm. For the purposes of this work the strain-gradient force will be noted in units of the equivalent electric field, even though no net charge is actually transported. Quite simply, an equivalent electric field of 0.2 V/cm corresponds to a gradient in the band gap of 0.2 eV/cm. Although the strain-gradient method is unable to produce the very large forces (up to 1 kV/cm) used in the usual transport experiments, gradients of up to 0.6 V/cm are readily attainable. These gradients are quite sufficient to produce $v_d\approx S$, due to the extremely high mobility of the droplets.

The work to be presented here consists of measurements of the mobility of the EHD as a function of strain-gradient force F_σ and temperature. Our principal goals are twofold: First is the investigation of near-sonic conduction. The high purity of the Si crystal eliminates all but carrier-phonon scattering contributions to momentum damping. The photoluminescence technique permits EHD detection without the use of external probes and allows spectroscopic characterization of the conducting system while it is actually in motion. The properties of EHD permit us to study a transport regime that is otherwise very difficult to assess.

Second, the measurements of drop mobility are valuable to the study of the electron-hole-droplet system itself. The carrier-phonon scattering time is a fundamental property of this unique fluid. The classic Bloch conductivity theory predicts very rapid decrease in damping ($\tau\propto T^{-5}$) at sufficiently low temperature, compared to $\tau\propto T^{-1}$ at higher T. Observation of this rapid temperature dependence would confirm the nature of the phonon scattering with a Fermi liquid and allow comparison of scattering times with theory. In Ge the low-temperature regime begins below 1 K, beyond the range of experiments to date. However, in Si the T^{-5} regime is entered below about 4 K, which is easily obtainable in a standard ^{4}He cryostat. Thus we can hope to study the fundamental interaction of thermal phonons with a new Fermi system.

For both Si and Ge it has been shown that in unstrained material, the transport of EHD is dominated by a "phonon-wind" force produced by phonons emitted during thermalization of the photoexcited carriers.[13,16] Some previous results, for laser-pulse-excited Ge, have suggested that droplet transport at velocities as high as 2×10^6 cm/sec is possible.[17,18] In contrast, several theories predict that an increase in carrier-phonon coupling near the speed of sound prohibits supersonic drop motion.[19,20] Our experiments examine this high-velocity EHD transport regime.

II. EXPERIMENTAL METHOD

The conduction-band structure of Si near its energy gap consists of a sixfold-degenerate conduction band with minima along the ⟨100⟩ axes. The valence band, centered at the Γ point ($k=0$), is twofold degenerate at $k=0$ and is composed of light- and heavy-hole bands. When crystal strain is applied along the [100] axis, the two conduction-band

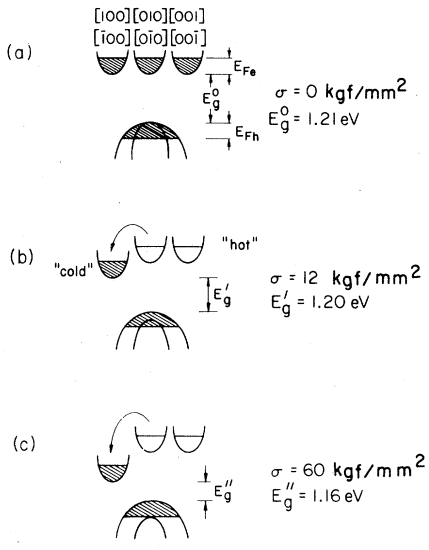

FIG. 1. Schematic diagram showing the effects of uniaxial strain on the conduction and valence bands of Si. The shaded regions indicate states occupied by the EHL. (a) Bands with no stress; all the conduction bands are equally populated, (b) $\sigma\simeq12$ kgf/mm^2 (1 kgf/mm^2=1 MPa); the Fermi energy of EHL in the lowered conduction bands lies below the minima of the raised bands, (c) $\sigma=60$ kgf/mm^2; the hole band is fully split, leaving only the heavy-hole-band populated. Electrons in the upper bands thermalize to the lower-energy band with intervalley relaxation time τ_I. Those remaining may form a "hot" EHL occupying the raised bands.

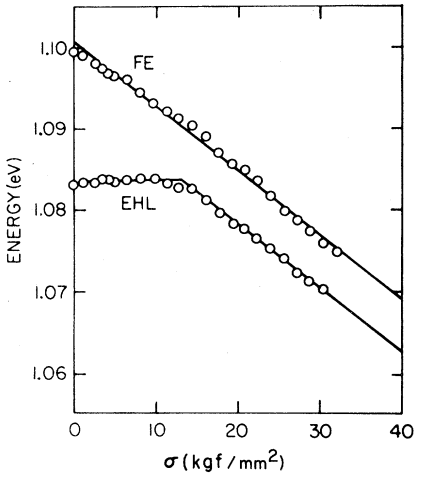

FIG. 2. Energies of the FE and EHL emission peaks as a function of stress. The EHL energy begins to shift as σ exceeds 12 kgf/mm^2 (from Ref. 21). Our drift experiments are all conducted in the linear region above 12 kgf/mm^2.

minima along that direction are lowered in energy, while the remaining four are slightly raised (Fig. 1). Also, the valence-band degeneracy is lifted. The strain effectively reduces the energy gap of the semiconductor. When the strain is sufficiently large ($\sigma \gtrsim 12$ kgf/mm^2; 1 kgf/mm^2=1 MPa) the splitting of the conduction band will exceed the Fermi energy of the EHL.[21] This will produce an EHL occupying only the two lowered conduction bands. Above this minimum strain, the conduction-band split widens and the valence bands continue to separate. The total energy of the EHL is continuously reduced with stress. Figure 2 illustrates this effect by plotting the peak positions of the EHD and FE spectrum lines as a function of σ. Any inhomogeneity in strain will produce a gradient in total electron-hole-pair energy, and therefore a net force on the liquid. It is this strain-gradient force that is used in place of an applied voltage for our transport studies.

The strain-gradient force has been used before in studies of the thermodynamics of the carriers confined to a region of maximum strain.[21] The strain maximum produces a potential minimum called the strain well.[22,23] We previously reported the transport of free excitons in Si using the gradient in strain from the sample surface to the strain well.[14] That experiment demonstrated that the proper choice of geometry can produce a uniform strain-gradient force over a distance up to 0.5 mm.

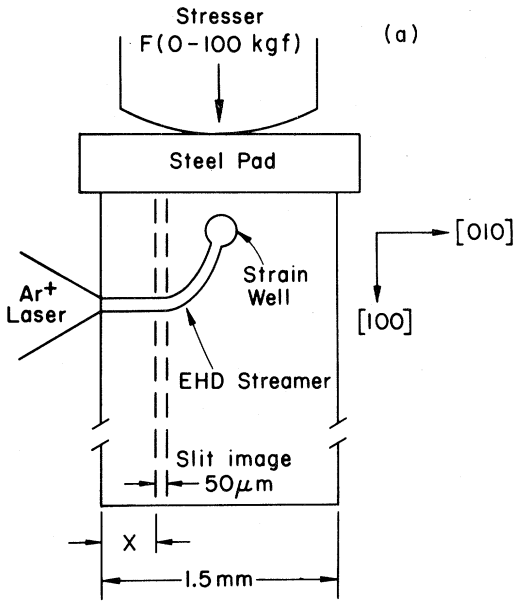

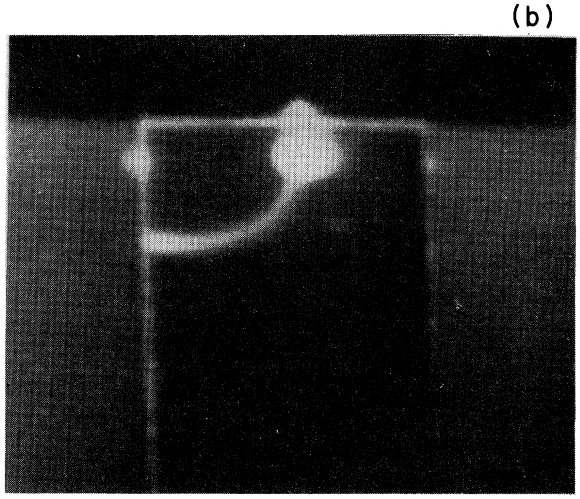

FIG. 3. (a) Sample and stresser configuration for the drift experiments. EHD (or FE) are photoexcited at the sample surface $x=0$ and drift down the strain-induced energy gradient. The steel pad was included to maintain a large uniform stress component when small gradients were desired. The slit image corresponds to a 50 μm spatial resolution. (b) Vidicon image of an optimized EHD streamer at $T=2.0$ K and $P_{abs}=300$ mW. The stress maximum below the stresser was approximately 50 kgf/mm^2.

The present experiment is divided into two phases: the generation and calibration of a strain-gradient force, and the measurement of the EHD drift velocity. The sample was an ultrapure ($N_A - N_D < 10^{12}$ cm^{-3}) dislocation-free Si crystal

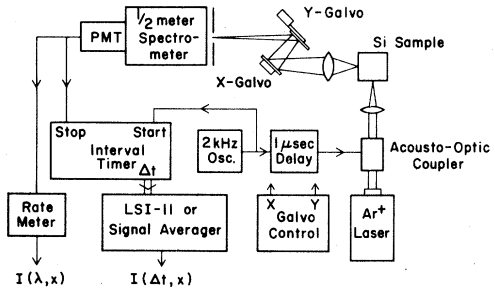

FIG. 4. Block diagram of the experimental apparatus. The galvo displacements could be controlled manually or by the LSI-11. The data could be directly displayed on an x-y recorder and stored on floppy disk media.

$1.5\times1.4\times4.0$ mm^3. All the edges were along $\langle 100\rangle$ axes. A section cut from a 7.6 cm diameter steel ball bearing was pressed against the top of the sample, as in Fig. 3(a). The sample was cooled in a liquid-helium immersion cryostat. The electron-hole pairs were generated by 100 to 200 mW of incident Ar^+-laser light ($\lambda=0.51$ μm). The laser was focused to a spot ~ 70 μm in a diameter to optimize EHL production. The recombination light emitted as the liquid decayed was collected by an 85-mm f/1.4 lens. A $5\times$-magnified image of the sample was focused onto the entrance slitplane of a $\frac{1}{2}$-meter spectrometer, as shown in Fig. 4. The image could be continuously displaced horizontally and vertically across a 250 μm entrance aperture, corresponding to a 50 μm square aperture on the crystal. This allowed precise control over whichever region of the crystal was sampled.

The spectrometer output was detected by a special nitrogen-cooled ir-sensitive photomultiplier tube (Varian VPM-164). The discriminated pulse output from the tube was directed to two devices: a rate meter with analog output proportional to the photon count rate and a sixteen-channel interval timer (Fig. 4). This timer, constructed in our laboratory, was capable of recording with 10-nsec resolution the delay time between a "start" signal and the detection of photons by the photomultiplier tube. The arrival of up to sixteen photons following the start pulse could be accommodated. The timer system sequentially sent the recorded delay times to a signal averager or an LSI-11 minicomputer for recording in a histogram form. Also, an ir Vidicon camera provided a continuous image of the recombination light without spectral resolution.

Force was applied to the ball bearing through a stiff automobile valve spring which was compressed by a micrometer drive. This permitted application of reproducible uniaxial forces up to 100 kgf. With force applied and the laser excitation on continuously (cw), the vidicon image was used to optimize the EHD drift path. Figure 3(b) is a photograph of an optimized EHD "streamer." The laser spot was so positioned as to produce the longest possible linear path for the drops.[24] It was along this straight segment that the drift velocities were measured.

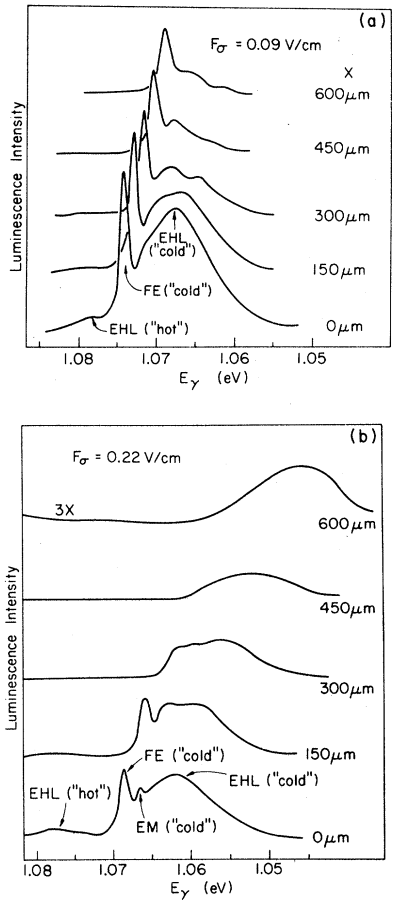

FIG. 5. Two series of recombination spectra taken at successive x positions along the EHD streamer at $T=2.0$ K. The loss of EHD intensity is consistent with the measured velocity and an EHD lifetime of about 150 nsec (Ref. 35). (a) $F_\sigma=0.09$ V/cm, (b) $F_\sigma=0.22$ V/cm. An excitonic molecule (EM) line is visible 2.5 meV below the FE in both sets of spectra. At higher gradients the FE line grows broader as it moves into the sample, possibly due to heating of the exciton gas.

With cw excitation, a series of spectra were then taken at 150 μm intervals along the streamer. Figures 5(a) and 5(b) show two sets of spectra. Both free-exciton (FE) and the very broad EHD peak are

seen. The two peaks shift together to longer wavelengths as regions deeper in the crystal are sampled. This energy shift directly produces the energy gradient without requiring a knowledge of the actual strain field or deformation potentials. Uniaxial strain also has the effect of reducing the density of the electron-hole liquid. In Ref. 21 it was shown that for stresses greater than 30 kgf/mm^2 the pair density is nearly independent of strain. In this range, the EHL density n_0 is roughly 5×10^{17} cm^{-3}. To prevent any change in the properties of the EHD during the mobility measurements, the strain gradients were always generated in such a way that the stress at the sample surface was greater than 30 kgf/mm^2. When small gradients were desired, a stainless-steel or tool steel plate was inserted between the stresser bearing and the sample. This allowed the creation of relatively small strain gradients while satisfying the requirements for a large initial strain. The success of these experiments relied upon the ability to vary the strain gradient over a wide range ($0.04<F_\sigma<0.6$ V/cm).

Once the desired strain gradient was achieved the laser was chopped by an acousto-optic coupler with a 15 nsec rise time (10–90%). The laser was switched on for only 2–10 μsec at a relatively slow rate of 2–10 kHz. This prevented sample heating and allowed the computer or signal averager time for data processing.

The signal to the acoustic-optic (A-O) switch was delayed relative to the interval timer start signal so that the timer was already running when the laser went on. With the spectrometer set to the FE or EHD wavelength appropriate to the chosen x position, a delay-time histogram was built up. Figure 6 is part of a series of such histograms at 150 μm intervals in x, showing the increasing delay in arrival time at successive x positions. The display data of Fig. 6 were accumulated by the LSI-11 which required $\sim$100 μsec to handle each photon count. The signal averager required only 7 μsec, producing a great increase in efficiency and in signal-to-noise ratio. For the purposes of actual velocimetry, the faster device was used, producing much clearer buildup signals than those shown here. Each histogram represents 512 sec of data accumulation. The shift in delay time and the known travel distance give the EHD drift velocity. With both the drift velocity and the applied force in hand, the mobility $\mu=v_d/F_\sigma$, is directly determined. For a total e-h pair mass, $m=m_{et}+m_h$, the momentum damping time is given by the drift relation

$$\tau=(m_{et}+m_h)v_d/F_\sigma\ . \tag{2}$$

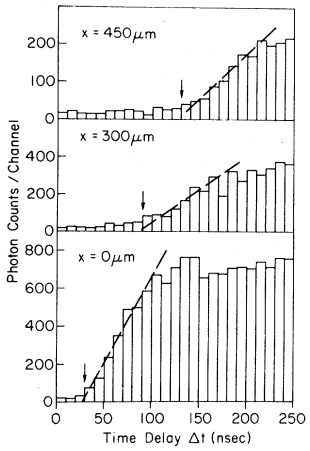

FIG. 6. Histograms of the time buildup of the EHD signal at three x positions, corresponding to Fig. 5(b). The onset was defined as the time at which the EHD signal first rises above the background.

Figure 6 displays EHD signals that appear to rise to their steady-state value in about 70 nsec. This time is much greater than the 15-nsec risetime of the A-O switch. When measured by the PMT and the interval timer (rather than a fast photodiode) the A-O device showed an apparent risetime of 30 nsec. At $x=0$ both the FE and EHL signals showed the same 70-nsec risetime. Because this time does not increase as the carriers move into the sample, we conclude that it is not a diffusion effect. Thus we tentatively assign this 70-nsec time constant to the initial equilibration time of the FE and EHD. Equilibration times of this magnitude have been reported previously.[25,26]

III. RESULTS: FREE EXCITONS

In the first experiments to use the calibrated-strain-gradient method in Si, we measured the momentum damping time of FE for $1.3<T<30$ K.[14] In these experiments a drift relation ($v_d\propto F_\sigma$) was confirmed over the full range of accessible forces $0<F_\sigma\lesssim0.4$ V/cm. However, the time resolution of that experiment was somewhat poorer than in the present EHD drift experiment; the acousto-optic coupler we used had a 150-nsec 10%–90% risetime. This limited the maximum velocity that could be reliably resolved to $\sim2\times10^5$ cm/sec. The steel stress pad was omitted in order to *minimize* the surface strain. This kept the surface strain below the critical $\sigma=12$ kgf/mm^2 (see Fig. 2), confining any EHD generated to a region near the sample surface. Thus only FE were drawn down the strain gradient for the velocity determination.

The momentum damping time τ was found to vary as $T^{-3/2}$. This dependence is characteristic of acoustic phonon-carrier scattering. The relation holds down to $T=1.3$ K, indicating that phonon scattering still dominates carrier transport near 1 K, a testament to the high purity of the silicon. The magnitude of the scattering time (in sec)

$$\tau=(8.8\pm0.5)\times10^{-10}/T^{3/2} \tag{3}$$

was in very good agreement with the estimate[26] (in sec)

$$\tau_p=\frac{2\sqrt{2}}{3}\pi\frac{\rho s^2\hbar^4}{m^{3/2}D^2}(kT)^{-3/2}=2\times10^{-9}T^{-3/2}\,. \tag{4}$$

In this estimate for Si, $m=m_{et}+m_{ht}=0.45m_0$, $\rho=2.3$ g/cm^3, the sound velocity $S=6\times10^5$ cm/sec, and the total of the electron and hole deformation potentials $D\simeq4$ eV.[26] Both the measured and estimated values of τ are sensitive to the choice of hole mass [see Eq. (2)]. A calculation of effective mass as a function of strain was performed by Kelso.[25] Those results indicate that the hole mass for excitons is in the high-strain limit at these low temperatures ($m_h=m_{ht}=0.26m_0$).

The good quantitative agreement between theory and experiment is a strong indication of the validity of the deformation-potential model of carrier-phonon scattering. In that model the energy shift of a carrier due to a phonon-associated crystal strain is taken as identical to the shift due to a static strain of the same magnitude. The effectiveness of the scattering calculation for FE lends credence to those performed for EHD by the same methods. Thus in examining EHD transport, large deviations from the scattering model (such as when $v_d\approx S$) are likely to signify a real change in scattering dynamics, rather than an error in the basic deformation-potential model itself.

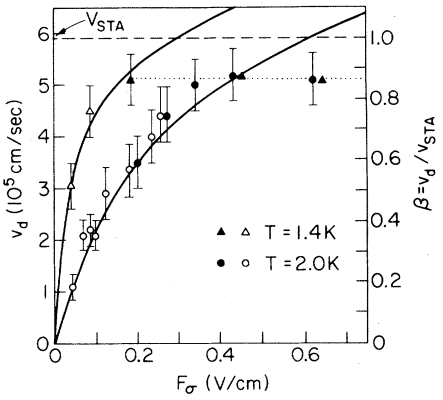

FIG. 7. Force dependence of the EHD drift velocity at $T=1.4$ and 2.0 K. The open symbols indicate the use of a steel pad to reduce the strain gradient, and solid symbols denote data taken without the pad. The solid lines are the scaled results of the theory of Ref. 30. Notice that the 1.4-K data exhibit a strong saturation in drift velocity above $F_\sigma=0.2$ V/cm (dotted line).

IV. RESULTS: EHD

The electron-hole liquid is a degenerate condensed phase of electrons and holes. Because thermal phonon scattering at low drop velocity may only include carriers near the Fermi surface, most of the carriers in a drop are unable to scatter. Just as in a conducting metal, the high density of carriers and the exclusion principle greatly enhance the average carrier mobility. Thus the EHD are expected to be more mobile than free excitons at the same temperature.

The EHD drift velocity was first measured at $T=1.4$ and 2.0 K with F_σ ranging from 0.04 to 0.6 V/cm. The resulting velocities are shown in Fig. 7. For this work the drift velocity is noted as $\beta=v_d/S$ where S is the velocity of the slow transverse-acoustic phonon (STA) in the ⟨100⟩ direction ($v_{STA}=S=5.9\times10^5$ cm/sec). The EHD momentum damping time and the equivalent droplet mobility are shown in Fig. 8. In the 2.0-K data the velocity is linear with F_σ until $\beta\simeq0.5$. In this linear range, $\tau_{EHD}(2.0\text{ K})=0.6$ nsec. This is approximately twice the measured FE damping time, $\tau_{FE}(2.0\text{ K})=0.3$ nsec. We found it impossible to generate reproducible strain forces smaller than $F_\sigma=0.04$ V/cm. It is not clear from the data,

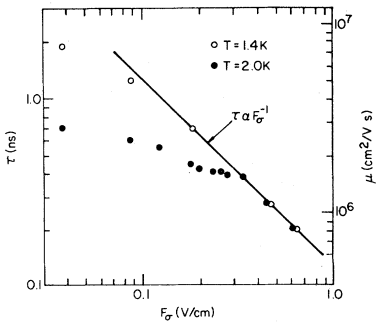

FIG. 8. Force dependence of the EHD momentum damping time and drift mobility at 1.4 and 2.0 K. Constant τ indicates linear damping. The F_σ^{-1} dependence in τ indicates velocity saturation. The scattering time is evaluated from the measured mobility using $\tau=\mu m$ and the pair-mass $m_{et}+m_{ht}=0.45m_0$.

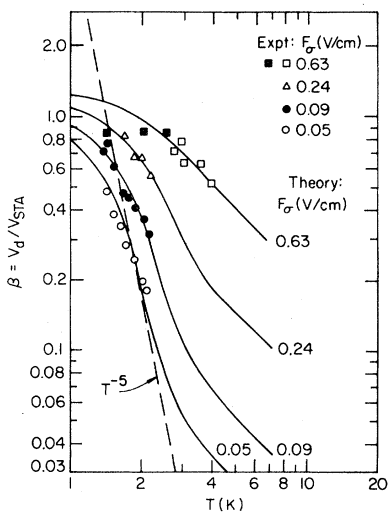

FIG. 9. Temperature dependence of β for several strain-gradient forces. The solid lines are the theory of Ref. 30, using the same scale factor as in Fig. 7.

therefore, at what strain force the drift velocity becomes nonlinear in F_σ at 1.4 K. Figure 8 clearly shows that the EHD mobility at 1.4 K is dependent upon F_σ throughout the entire range of strain-gradient forces. Assuming that the $F_\sigma = 0.05$ V/cm value is in the linear range will underestimate τ(1.4 K). This results in $\tau(1.4\text{ K}) = 1.8$ nsec. Thus at 1.4 K the droplets are over 3 times as mobile as the FE for which $\tau_{FE}(1.4\text{ K}) = 0.5$ nsec.

At drift velocities well below the sound speed the EHD are clearly more mobile than the FE. In addition, the mobility is increasing more quickly than $T^{-3/2}$ as the temperature is reduced. This rapid temperature dependence is an indication of the effect of the Fermi-liquid nature of EHD on its transport.

Both the 1.4 and 2.0-K results show a saturation in drift velocity near $\beta = 0.9$ ($v_d = 5.2 \times 10^5$ cm/sec). Indeed, Fig. 8 shows perfect saturation ($\tau \propto F_\sigma^{-1}$) at large forces: an increase in motive force produces no detectable increase in droplet velocity. This observation of an enhanced EHD-phonon coupling near $\beta = 1$ indicates that supersonic drop transport is not within reach of our experimental range of strain forces.

The drift velocity was measured as a function of temperature over the range $1.35 < T < 2.15$ K for $F_\sigma = 0.05$, 0.09, 0.21, and 0.63 V/cm. The results of these measurements are shown in Fig. 9. The highest strain force data indicate *no* temperature dependence in v_d for $1.4 < T < 2.5$ K. From Fig. 7 it is clear why this is so; within this range of temperatures the highly mobile droplets have v_d saturated near S. Figure 10 shows the temperature dependence of τ for each of the strain gradients. The low-gradient values appear to lie on a common curve, discussed in the next section. Velocity saturation appears as a saturation in τ. The open boxes in Figs. 9 and 10 indicate data for which sample heating may be inhibiting EHD transport, while enhancing FE production. These are lower limits to the EHD drift velocity, or possibly measures of the FE drift velocity. The remainder of the data were taken below the λ point of liquid He, where no sample heating was evident.

From Figs. 9 and 10, it is evident that the temperature dependence of v_d becomes more rapid when F_σ is made smaller. To state this another way, the drop mobility becomes more sensitive to temperature as the drift velocity is reduced. This is also evidence for an enhanced carrier-phonon coupling near $\beta = 1$. Taken as a whole, the data show a nonlinear drift relationship as v_d approaches S, and a saturation of v_d at 5.2×10^5 cm/sec, which corresponds to $\beta = 0.9$. A comparison of these observations with theory will now be made.

V. THEORETICAL CONSIDERATIONS

The effect of the finite drift speed on the Fermi system is to shift the center of the Fermi surface away from $v = 0$. On the parabolic momentum-energy diagram, this has the effect of removing car-

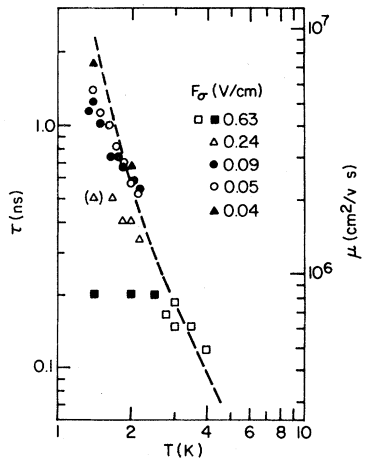

FIG. 10. Temperature dependence of the EHD momentum damping time and drift mobility. The dashed curve is Eq. (10) scaled to coincide with the data at 2 K. The data point in parentheses indicates a single measurement with lower reliability than the remainder of the data.

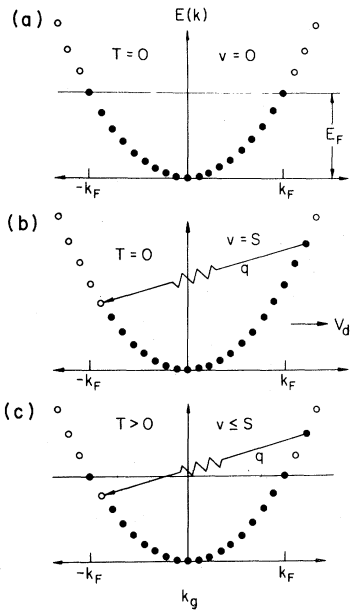

FIG. 11. Schematic momentum-energy diagram showing the effect of near-sonic velocity and finite temperature on EHD transport. The solid symbols indicate occupied states while the open symbols represent empty states. (a) At $T=0$ and $v_d \ll S$ phonon emission cannot connect a filled to an empty state; emission is impossible implying very high mobility. (b) At $T=0$ and $v_d=S$ the phonon can span the Fermi surface; forward phonon emission will strongly damp droplet motion. (c) At finite T, but $v_d<S$ a thermally excited carrier near $+k_F$ may move by phonon emission to a thermally vacated state near $-k_F$. Thus at finite T strong emission damping begins below the sound velocity.

riers from the $-k_F$ edge to the $+k_F$ edge of the Fermi surface. This is shown diagramatically in Fig. 11. Carriers with momenta along the drift direction populate states at higher energy, whereas high-energy states with momentum opposed to the drift are depopulated. When the drift velocity nears the phonon velocity, the phonon may directly connect the forward edge of the Fermi sphere to the trailing edge. Emission of a phonon will then carry the highest-energy carrier back to an empty state on the trailing edge. Even at $T=0$, this phonon emission will produce damping once $v_d=S$. However, at finite temperature there will already be some excited carriers on the forward side, and some vacant states to the rear. The damping will then begin to become nonlinear at some droplet velocity less than that of the phonons. Furthermore, the onset of the nonlinearity will move to smaller velocity as the carrier temperature is raised. Of course, this reduction in mobility will have a gradual onset at finite T, growing sharper as T is reduced.

The forward emission of phonons also may affect the effective carrier temperature within the drop. In the frame of reference moving with the drop, the phonon emission described has transferred a carrier from a state above the Fermi surface to one below it. Effectively, the drop is cooling by phonon radiation. It is possible that this radiation may actually drive the carrier temperature below that of the crystal itself.[3] Reference 3 estimates that this will be the case for subsonic droplet transport in Si for $T \lesssim 4$ K. We have no direct evidence for the possible cooling effect.

It can also be demonstrated that the absorption and directed reemission of thermal phonons is *required* for velocity damping at subsonic velocities. Assuming that all the energy that the drop acquires in moving down the strain gradient is emitted in the form of phonons, the rates of gain and loss of momentum can be equated. For a phonon emission at an angle θ with respect to the drift direction, the carrier momentum in the drift direction p_x changes by $\hbar q \cos\theta = \hbar\omega \cos\theta / S$. By this emission the droplet loses kinetic energy $\Delta E_d = \hbar\omega$. The phonon drag force resulting from phonon emission is

$$F_p = \frac{\partial p_x}{\partial t} = \frac{\langle \cos\theta \rangle}{S} \frac{\partial E_d}{\partial t} . \tag{5}$$

The energy lost to phonon emission must equal the energy from motion in the strain field:

$$\frac{\partial E_d}{\partial t} = \vec{F}_\sigma \cdot \vec{v}_d . \tag{6}$$

Setting $F_p = F_\sigma$, we then find

$$v_d = S / \langle \cos\theta \rangle . \tag{7}$$

No matter what the energy spectrum of the emitted phonons, the drift energy gain, emitted as phonons, is insufficient to prevent acceleration of the drop to supersonic velocity. The required damping force must come from redirection of thermal phonons. These phonons, with random propagation direction, are absorbed by the drop, and reemitted with a bias to the forward direction. It is at the equilibrium between the motive force and those two momentum-loss rates (emission and thermal redirection) that v_d is constant. The theory to be described determines as a function of velocity and temperature what strain-gradient force will exactly balance the phonon-damping force. Indeed, in this model, for large forces, the drift velocity may still become supersonic.

A detailed theory of the phonon-damping process is presented by D'yakonov and Subashiev.[30] Their calculation extends the original result of Keldysh[31] to include the effects of finite velocity. It also exactly reproduces the Keldysh result when $v_d \ll S$. By including the effects of finite drift velocity on the phonon absorption and emission rates, the nonlinear damping effects can be included in a calculation similar to that of Ref. 27. The final result is the force $F(\beta,T)$ necessary to maintain a reduced drift velocity $\beta = v_d/S$ at temperature T

$$F(\beta,T)=\frac{1}{(2\pi)^3}\sum_{i=e,h}\frac{m_i^2 D_i^2}{h^2\rho n_0}(2k_F)^5 I_i(\beta)\ , \tag{8}$$

where

$$I_i(\beta)=\frac{1}{(2k_F)^5\beta^2}\left[\frac{kT}{\hbar S}\right]^5\int_0^{z_0} z^4 dz\int_{1-\beta}^{1+\beta} dt\, t\frac{e^z-e^{zt}}{(e^{zt}-1)(e^z-1)}\ . \tag{9}$$

Here $z_0 = 2hSk_F/kT$, and $t = 1-\beta\cos\theta$ where θ is the angle of phonon momentum to the direction of droplet motion. It is easy to include the effect of a carrier temperature different from that of the lattice. A change in the EHD temperature can be accomodated by a scale factor in t. The authors of Ref. 30 include this effect in their calculation. It is omitted here, with little change in the final result.

At low velocity $\beta \ll 1$ the integrand may be expanded to first order in z, with the result

$$I_i(\beta)=\frac{2}{3}\frac{\beta}{(2k_F)^5}\left[\frac{kT}{\hbar S}\right]^5\int_0^{z_0}\frac{z^5 e^z}{(1-e^z)^2}dz\ . \tag{10}$$

The force is linear in β. This low velocity limit exactly reproduces the earlier result of Keldysh.[31] The temperature dependence of Eq. (10) is the same as the classic Bloch formula (cf. Ref. 27). The low-velocity Bloch-conductivity result, scaled to match the data at 2 K, is shown in Fig. 10. The form of the temperature dependence fits the data quite well. We can also show that the calculated magnitude is in reasonable agreement, despite the approximation of spherical bands.

For EHD in Si under the experimental stress conditions, $n_0 = 5\times10^{17}$ cm^{-3},[21] $D_e = -3.0$ eV, and $D_h = -6.8$ eV.[29] In the low velocity limit the calculation produces the results for EHD in Si: $\tau \simeq 3\times10^{-8}$ T^{-5} sec for $T \lesssim 4$ K. At 2 K the theory predicts $\tau = 1.0$ nsec, while $\tau = 0.6$ nsec was observed experimentally. In the higher velocity regime, the theory shows the same qualitative behavior as the data, but appears to overestimate the drop mobility. However, the use of a single scale factor brings $F(\beta,T)$ into agreement with experiment over the entire range of velocities and temperature observed, as discussed below.

D'yakanov and Subashiev also estimate damping rates for a Cherenkov-type emission of phonons where $v_d \geq S$.[30] This emission is not a direct carrier-phonon interaction. It is a result of the lattice deformation due to the presence of the high density of e-h pairs in a drop. This lattice deformation is carried along with the drop. At subsonic velocities phonon emission takes place only as the drop is accelerated, and vanishes when v_d is constant. However, the damping becomes finite for constant velocities above S, and decreases as $1/v_d^2$ thereafter. Thus the calculations do not preclude the possibility of supersonic droplet transport. They do indicate that the forces required to maintain a constant velocity grow very rapidly as the speed of sound is approached. Furthermore, the force required may increase discontinuously as S is exceeded. This type of velocity limit is strongly suggested by the data.

VI. DISCUSSION

The results of the calculations in Ref. 30 are presented in terms of a calculated force needed to maintain a chosen drift velocity. Using the parameters from the previous section, the predicted force is approximately 40% smaller than that observed. By scaling the calculated force by a single factor near unity, the estimates can closely approximate the actual data at both 1.4 and 2.0 K. The scaled theoretical curves appear in Fig. 7.

The small scaling discrepancy between experiment and theory may be rooted in the simplifying approximations of the theory. The theory does not include the effects of the anisotropy in the carrier masses, nor anisotropy in phonon velocity and phonon-carrier coupling. In addition, the screening effects of the high density of carriers within the drop are not included.

The best fit to the data does not produce the sharp velocity limit that was observed at $\beta = 0.9$. At 1.4 K, the velocity did not increase at all from $F_\sigma \simeq 0.16$ V/cm to $F_\sigma = 0.63$ V/cm, while the

theoretical curve continues to rise. The data appear to have the sharp cutoff associated with the "Cherenkov" emission, as well as the gradual saturation expected from the reemission damping at velocities below S. A simple explanation for the subsonic velocity limit ($\beta=0.9$ rather than $\beta=1.0$) may lie in the anisotropy of phonon velocities in the Si crystal. The initial explanation of the nonlinear damping assumed isotropic phonon velocity. This requires the first phonons emitted to be in the directly forward direction. However, an STA phonon propagating at a small angle to the $\langle 100 \rangle$ axes will have a lower velocity. The slower phonons emitted as the nonlinear damping regime is reached will radiate in a noncylindrical "cone" about the direction of motion. This would indicate that the Cherenkov phonon radiation is possible at subsonic droplet velocities. A simple estimate considering the phonon focusing of STA phonons near the $\langle 100 \rangle$ propagation direction, suggest that this effect could produce velocity saturation at $\beta=0.95$.

A Cherenkov-type conductivity limit would be unique to the EHD system. The coherent emission of phonons is due to displacement of the small volume of strained crystal within the drop itself. In a normal conducting system the carriers are distributed uniformly, and so do not produce spatial variations in crystal strain. In a normal conducting system one still might expect to observe a nonlinear velocity damping near and above the sound velocity, but no absolute limit to the achievable drift speed.

The theory of Ref. 30 may also be used to generate a family of curves of v_d vs T at selected values of F_σ. With the use of the same scale factor as before (Fig. 7), the theoretical curves corresponding to the experimentally measured forces are plotted in Fig. 9. The close correspondence of theory and experiment in the temperature dependences is further confirmation of the strong influence of nonlinear damping effects at subsonic velocities. The temperature dependence one observes is very sensitive to the motive force F_σ in the experiment. At the highest force (0.64 V/cm), the drift velocity is temperature independent (i.e., saturated as in Fig. 8) up to nearly 3 K and then falls weakly with increasing temperature. It is only for small driving forces that the droplet velocity exhibits the rapid temperature dependences usually expected for a degenerate Fermi liquid. At the smallest driving force (0.05 V/cm), the theoretical curve approaches the T^{-5} dependence (dashed curve in Fig. 9) characteristic of the linear-damping, low-temperature regime (see also Fig. 10). The experimental results show that the temperature dependence of the EHD momentum damping time is entirely characteristic of phonon scattering by a degenerate Fermi system.

An extension of these experiments to even lower velocities and temperatures would be very difficult. The saturated velocities are so easily achieved at low T that the production of extremely small forces is necessary. Since droplets live for less than a microsecond, low-velocity droplet transport is only observable over small distances near the excitation point. Indeed, at lower velocites it would be necessary to take into account other transport effects [e.g., phonon wind or exciton diffusion (see Ref. 14)]. The 0.05-V/cm gradient used here was the smallest we could achieve while satisfying the criteria for uniform gradient and large initial strain. Nevertheless, our experimental conditions did allow observation of the rapid T dependence of τ expected for a degenerate Fermi system.

VII. HOT EHL

When the strained Si crystal is photoexcited, the raised conduction bands are briefly occupied as well as the lower ones. The electrons falling into the upper bands will scatter to the lower bands in the intervalley scattering time τ_I. The carriers in the upper conduction bands contribute a "hot" component to the EHL.

The EHL in strained Ge also exhibits a hot component.[32] For that material, evidence has been reported that the mixed hot- and cold-carrier system can spatially phase separate.[33] It is believed that the phase of mixed hot and cold EHL (called phase II) has a constant hot-carrier density, but occupies a decreasing fraction of the drop volume as the hot electrons decay to the cold bands. The remaining fraction (phase I) contains only thermalized (cold) electrons and holes.

Because the phase-separated component (phase II) has a lower energy than would a homogeneous liquid, the mixed phase is physically bound to the cold liquid comprising the remainder of the drop. Such a binding was demonstrated spatially in Ge.[15] In that experiment drops containing both hot and cold electrons were observed to move in a strain gradient. The hot component moved with the cold even through it was subject to an opposing strain-gradient force. This does not prove that a phase separation has taken place, but only that the energy of dissociation of hot and cold carriers, due to a phase separation *or surface energy,* is greater than that available from the strain-gradient force.

For Si, theory predicts that a similar hot-cold phase transition is extremely unlikely.[34] In this case the hot EHL should not be strongly bound to the cold, and may be spatially separable. Our experiments seem to bear out this prediction. The results are qualitatively very different from those in Ge. In no case in the Si experiments was hot EHL observed more than 150 μm into the sample. Even when detected at a close distance of $x=150$ μm the hot signal was only a small fraction of that at the sample surface $x=0$ μm.

This observation cannot be explained simply by intervalley conversion during the time it takes droplets to drift this distance. For pure Si under a uniform strain less than ~ 25 kgf/mm^2, τ_I was found to be 360 nsec.[35] In our drift experiments, had the hot EHL been moving with the cold, its luminescence would have been detected at far greater distances into the sample. Thus neither a phase-separation energy nor a surface energy is sufficient to hold the mixed drop together. This provides spatial evidence that there is no phase separation of a mixed hot and cold EHL for stresses near $\sigma=30$ kgf/mm^2 and $T=2$ K. This conclusion has previously been indicated by spectroscopic methods in Ref. 36.

VIII. CONCLUSIONS

The momentum damping time of electron-hole droplets in Si has been examined on a quantitative basis. For small motive forces where the drift velocity is well below the sound velocity, the damping time $\tau=mv_d/F$ is constant. For larger forces, as v_d approaches the sound velocity, the damping time decreases, causing a velocity limit of $v_d=5.2\times10^5$ cm/sec ($\beta=0.9$). Lowering the sample temperature increases the mobility for low speeds, but the same velocity limit is seen. For $\beta<0.9$, the temperature and force dependence of v_d is consistent with a thermal-phonon scattering model of droplet-momentum damping. The measured damping rate τ^{-1} is actually only 40% greater than the rate calculated, while a single scale factor can bring all of the data into agreement with theory. This is a dynamical confirmation of the Fermi-liquid nature of EHD, and a demonstration that phonon scattering dominates EHD transport at these low temperatures.

The strict velocity saturation that we have observed is not predicted in the thermal-phonon scattering model. It is possible that the droplet heats rapidly as β approaches 1, limiting the mobility, but this was not observable in the luminescence spectra, and theory predicts exactly the opposite effect.[3] A phonon-gain effect, like the effect observed in Refs. 6 and 10, is also possible. However, this is unlikely as the drops occupy only a small fraction of the material (unlike a uniformly occupied conductor). Most emitted phonons will not encounter another drop before leaving the droplet stream. On the other hand, a "sound barrier" is consistent with the prediction of coherent emission of phonons when $\beta\geq1$. A Cherenkov-type emission of phonons would be unique to the EHD system. Observations of a directed phonon flux emanating from the EHD stream would support this interpretation of our data.

ACKNOWLEDGMENTS

We wish to thank E. E. Haller for supplying the Si crystal, M. V. Klein for the loan of the special photomultiplier tube, F. Steranka for construction of the photon-timing system, and K. Hess for useful discussions. This project was supported by the National Science Foundation under the Materials Research Laboratory Grant No. DMR-80-20250.

[1]C. Kittel, *Introduction to Solid State Physics* (Wiley, New York, 1976), p. 171.
[2]J. C. Hensel, Phys. Lett. 4, 38 (1963).
[3]R. W. Smith, Phys. Rev. Lett. 9, 87 (1962).
[4]M. I. D'yakonov and A. V. Subashiev, Zh. Eksp. Teor. Fiz. Pis'ma Red. 27, 692 (1978) [JETP Lett. 27, 657 (1978)].
[5]A. R. Hutson, J. H. McFee, and D. L. White, Phys. Rev. Lett. 7, 237 (1961).
[6]A. B. Pippard, Nature (London) 8, 161 (1964).
[7]H. Heinrich and W. Jantsch, Phys. Rev. Lett. 57, 485 (1976).
[8]D. K. Ferry, J. R. Barker, and C. Jacoboni, in *Physics of Nonlinear Transport in Semiconductors, NATO Advanced Study Institute Series* (Plenum, New York, 1980).
[9]C. A. Nanney, Bull. Am. Phys. Soc. 11, 258 (1966).
[10]M. Pomerantz, Phys. Rev. Lett. 13, 308 (1964).
[11]J. C. Hensel, G. A. Thomas, T. G. Phillips, and T. M. Rice, in *Solid State Physics,* edited by H. Ehrenreich, F. Seitz, and D. Turnbull (Academic, New York, 1978), Vol. 32.

[12]Jagdeep Shah, M. Combescot, and A. H. Dayem, Phys. Rev. Lett. 38, 1497 (1977); A. Forchel, B. Laurich, B. Laurich, G. Moersch, W. Schmid, and T. L. Reinecke, *ibid.* 46, 678 (1981).

[13]M. A. Tamor and J. P. Wolfe, Phys. Rev. B 21, 739 (1980).

[14]M. A. Tamor and J. P. Wolfe, Phys. Rev. Lett. 44, 1703 (1980).

[15]M. A. Tamor and J. P. Wolfe, Phys. Rev. B 24, 3596 (1981).

[16]M. Greenstein and J. P. Wolfe, Phys. Rev. Lett. 41, 715 (1978).

[17]T. C. Damen and J. M. Worlock, in *Proceedings of the Third International Conference on Light Scattering in Solids,* edited by M. Balkanski, R. C. Leite, and S. P. Porto (Flammarion, Paris, 1976), pp. 183–188.

[18]N. V. Zamkovets, N. N. Sibel'din, V. B. Stopachinskii, and V. A. Tsvetkov, Zh. Eksp. Teor. Fiz. 74, 1147 (1978) [Sov. Phys.—JETP 47, xxxx (1978)].

[19]D. S. Pan, D. L. Smith, and T. C. McGill, Phys. Rev. B 17, 3284 (1978).

[20]V. S. Bagaev, M. M. Borch-Osmolovsky, T. I. Galkina, L. V. Keldysh, and A. G. Poyarkov, Proceedings of the 15th International Conference on the Physics of Semiconductors, Kyoto, 1980 [J. Phys. Soc. Jpn. 49, 495 (1980), Suppl. A p. 495].

[21]P. L. Gourley and J. P. Wolfe, Phys. Rev. Lett. 40, 526 (1978); Phys. Rev. B 20, 3319 (1979); 24, 5970 (1981); 25, 6338 (1982).

[22]R. S. Markiewicz, J. P. Wolfe, and C. D. Jeffries, Phys. Rev. B 15, 1988 (1977).

[23]J. P. Wolfe, R. S. Markiewicz, S. M. Kelso, J. E. Furneaux, and C. D. Jeffries, Phys. Rev. B 18, 1479 (1978).

[24]It should be noted that this photograph is different from the one previously published by P. L. Gourley and J. P. Wolfe [Phys. Rev. B 20, 3319 (1979)]. The earlier photograph shows exciton luminescence from a similarly strained Si crystal at $T=10$ K. The exciton "streamer" is much broader than that for droplets because of the far greater diffusivity of the FE.

[25]W. Schmid, Sol. State Commun. 19, 347 (1976).

[26]J. Shah and A. H. Dayem, Phys. Rev. Lett. 37, 861 (1976).

[27]J. M. Ziman, *Electrons and Photons* (Oxford University Press, Oxford, 1960).

[28]S. M. Kelso, Phys. Rev. B 25, 1116 (1982).

[29]I. Balslev, Phys. Rev. 143, 636 (1966).

[30]M. I. D'yakonov and A. V. Subashiev, Zh. Eksp. Teor. Fiz. 75, 1943 (1978) [Sov. Phys.—JETP 48, 980 (1978)].

[31]L. V. Keldysh and S. G. Tikhodeev, Zh. Eksp. Teor. Fiz. Pis'ma Red. 10, 582 (1975) [JETP Lett. 21, 273 (1975)].

[32]H.-L. Chou, G. K. Wong, and B. J. Feldman, Phys. Rev. Lett. 39, 959 (1977).

[33]G. Kirczenow and K. S. Singwi, Phys. Rev. B 20, 4171 (1979).

[34]G. Kirczenow, Phys. Rev. B 23, 1902 (1981).

[35]J. Wagner, W. Schmid, and R. Sauer, Solid State Commun. 32, 1215 (1979).

[36]J. Wagner, W. Schmid, and A. Forchel, Solid State Commun. 36, 917 (1980).

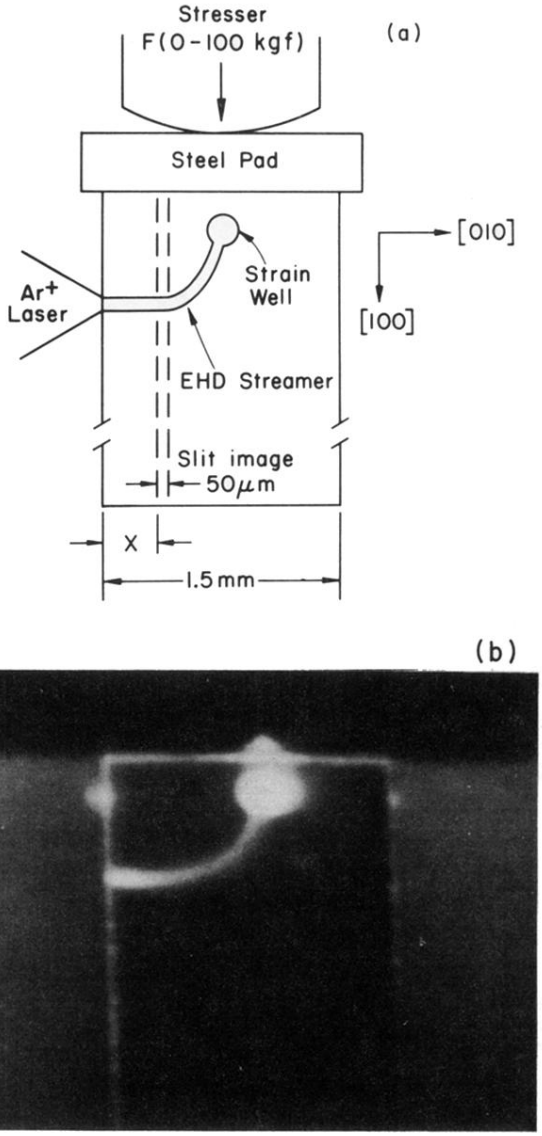

FIG. 3. (a) Sample and stresser configuration for the drift experiments. EHD (or FE) are photoexcited at the sample surface $x=0$ and drift down the strain-induced energy gradient. The steel pad was included to maintain a large uniform stress component when small gradients were desired. The slit image corresponds to a 50 μm spatial resolution. (b) Vidicon image of an optimized EHD streamer at $T=2.0$ K and $P_{abs}=300$ mW. The stress maximum below the stresser was approximately 50 kgf/mm^2.